

High pressure Laue diffraction and its application to study microstructural changes during the $\alpha \rightarrow \beta$ phase transition in Si

D. Popov, C. Park, C. Kenney-Benson, and G. Shen

Citation: *Review of Scientific Instruments* **86**, 072204 (2015); doi: 10.1063/1.4926894

View online: <http://dx.doi.org/10.1063/1.4926894>

View Table of Contents: <http://scitation.aip.org/content/aip/journal/rsi/86/7?ver=pdfcov>

Published by the *AIP Publishing*

Articles you may be interested in

Strength and structural phase transitions of gadolinium at high pressure from radial X-ray diffraction

J. Appl. Phys. **116**, 243503 (2014); 10.1063/1.4904747

High pressure-induced structural phase transition in hexagonal CeF₃ nanoplates

J. Appl. Phys. **111**, 112627 (2012); 10.1063/1.4726253

Phase transition and chemical decomposition of hydrogen peroxide and its water mixtures under high pressures

J. Chem. Phys. **132**, 214501 (2010); 10.1063/1.3429986

High pressure phase transition study of B–C–N compound

J. Appl. Phys. **107**, 073508 (2010); 10.1063/1.3369279

High-pressure x-ray diffraction study on the structure and phase transitions of the defect-stannite ZnGa₂Se₄ and defect-chalcopyrite CdGa₂S₄

J. Appl. Phys. **104**, 063524 (2008); 10.1063/1.2981089

Frustrated by old technology?

Is your AFM dead and can't be repaired?

Sick of bad customer support?

It is time to upgrade your AFM

Minimum \$20,000 trade-in discount for purchases before August 31st

Asylum Research is today's technology leader in AFM

dropmyoldAFM@oxinst.com

OXFORD
INSTRUMENTS
The Business of Science

High pressure Laue diffraction and its application to study microstructural changes during the $\alpha \rightarrow \beta$ phase transition in Si

D. Popov,^{a)} C. Park, C. Kenney-Benson, and G. Shen

High Pressure Collaborative Access Team, Geophysical Laboratory, Carnegie Institution of Washington, Argonne, Illinois 60439, USA

(Received 27 February 2015; accepted 10 May 2015; published online 20 July 2015)

An approach using polychromatic x-ray Laue diffraction is described for studying pressure induced microstructural changes of materials under pressure. The advantages of this approach with respect to application of monochromatic x-ray diffraction and other techniques are discussed. Experiments to demonstrate the applications of the method have been performed on the $\alpha \rightarrow \beta$ phase transition in Si at high pressures using a diamond anvil cell. We present the characterization of microstructures across the α - β phase transition, such as morphology of both the parent and product phases, relative orientation of single-crystals, and deviatoric strains. Subtle inhomogeneous strain of the single-crystal sample caused by lattice rotations becomes detectable with the approach. © 2015 AIP Publishing LLC. [<http://dx.doi.org/10.1063/1.4926894>]

INTRODUCTION

Laue diffraction using a polychromatic x-ray beam is often used to study crystal structures and microstructures of materials. It is sensitive to subtle changes in crystal orientation, deformation, and strain. Although the technique has been widely implemented to study materials at ambient pressure, for instance, to characterize mechanisms of their deformation,¹⁻³ it is desirable to apply it in characterizing materials under high pressure conditions. Even though potential outcomes from Laue diffraction in the high pressure regime have been demonstrated theoretically, its practical applications to this area are still limited.^{1,4} The Laue diffraction approach has clear advantages over monochromatic beam diffraction in several areas. For instance, a comparable number of Laue reflections can be collected much faster than monochromatic reflections by one or two orders of magnitude, which makes polychromatic x-ray diffraction much more useful for time-resolved measurements. Monochromatic beam diffraction can be used at high pressure to characterize the parameters of microstructure including the relative orientation of crystalline grains, morphology, strain, and dislocations.⁵ However, the tedious data collection in the monochromatic approach often obscures time dependent information. Moreover, the microstructural heterogeneity of most samples makes it necessary to collect spatially resolved, as well as time resolved, diffraction data together. Getting spatially resolved information in turn requires collection of translational scans with focused beam which also requires efficient data collection. Another important advantage of polychromatic beam diffraction is that there is no need to rotate the sample, which is particularly advantageous for high pressure experiments, because the sample rotation is often limited by the accessible opening angles of the high pressure device. This also eliminates the problem of

rotational stage eccentricity, significantly improving spatial resolution, in particular when submicrometer X-ray beams are used.

In this paper, we describe a polychromatic x-ray diffraction technique suitable for high pressure studies. Transmitted experimental geometry with incident X-ray beam perpendicular to the area detector plane is currently implemented because of the limited access angle of many high pressure devices such as using cryostats or externally heated furnaces.

We have applied the established Laue technique for characterizing microstructural changes during the $\alpha \rightarrow \beta$ phase transition in Si and have obtained information on the kinetics of the pressure induced phase transition. At about 13 GPa, Si exhibits a phase transition from a low pressure cubic α -phase to a tetragonal high pressure β -phase⁶⁻⁹ with coexistence of these phases in a narrow pressure range.^{7,9} The transition is accompanied by a large volume collapse of about 21%⁹ and a drastic drop in resistivity indicating a shift towards metallic bonding.^{6,7} Observations using infrared microscopy indicate a nucleation and growth mechanism because the high pressure phase appears locally and spreads through the sample.¹⁰ It is interesting to note that while this phase transition is strongly first order, dynamical coexistence of the β phase with the parent α phase was recently observed.¹¹ Currently, the most comprehensive microstructural information about structural phase transitions can only be obtained by studying the sample after quenching using X-ray diffraction combined with electron and optical microscopy.¹²⁻¹⁵ However, the study of recovered samples is applicable only if the microstructural features of interest are recoverable to ambient pressure. In this work, X-ray micro diffraction was applied *in situ* in order to get spatially resolved structural information during the phase transition at high pressures.

EXPERIMENTS

Polychromatic x-ray diffraction measurements have been conducted using the experimental setup at 16-BM-B of the

^{a)}Author to whom correspondence should be addressed. Electronic mail: dpopov@carnegiescience.edu

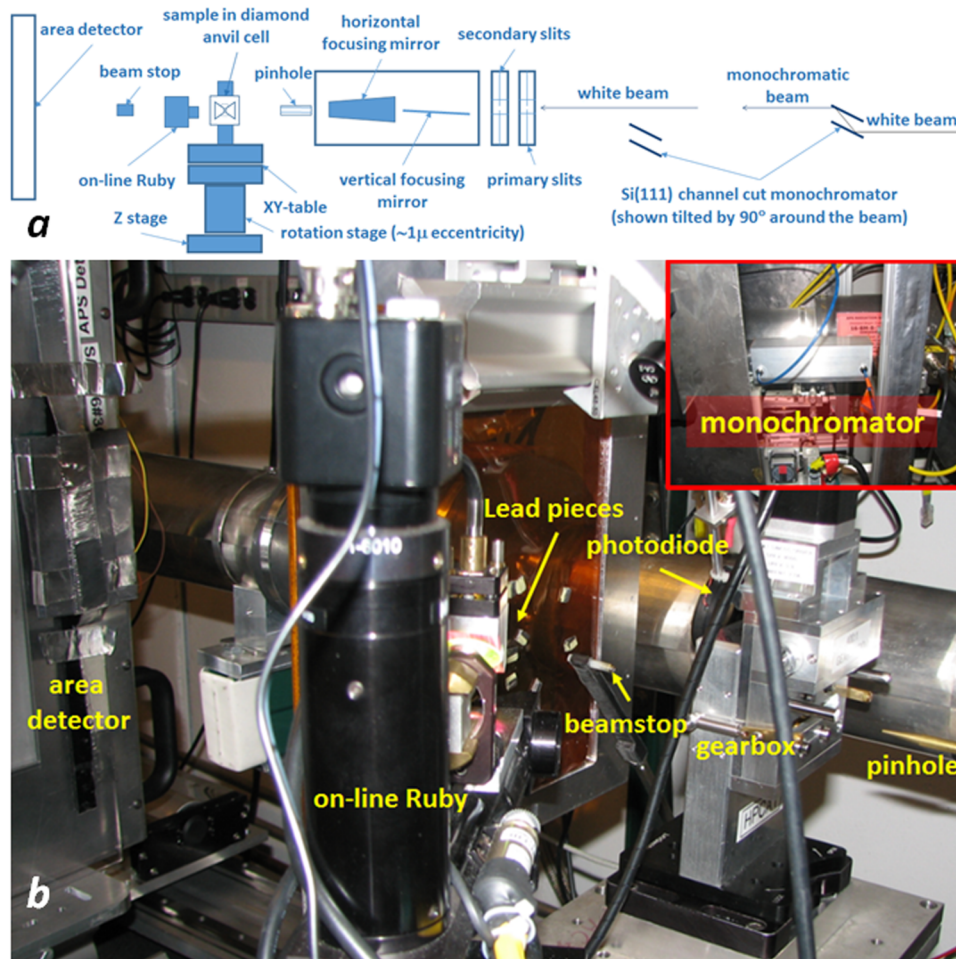


FIG. 1. Schematic (a) and photograph (b) of polychromatic x-ray diffraction setup at APS 16-BM-B beamline.

High Pressure Collaborative Access Team (HPCAT) sector at the Advanced Photon Source (APS) (Fig. 1). An X-ray beam with energies ranging from 5 to 70 keV was focused down to $7\text{--}9\ \mu\text{m}^2$ at FWHM using 200 mm Rh-coated Si Kirkpatrick-Baez (KB) mirrors. Diffraction patterns were collected with a Perkin Elmer area detector oriented perpendicular to the X-ray beam and offset so that the direct beam passed about 3 cm from one edge of the detector without striking it. A Si(111) channel cut monochromator provided monochromatic X-rays with a wavelength of $0.3065\ \text{\AA}$. The monochromator can be inserted, when needed, with only a few minutes of alignment time, allowing white beam/mono beam operations in an exchangeable manner. The sample to detector distance and detector tilt angles were calibrated using Fit2d software^{16,17} based on the diffraction image from a CeO_2 standard collected with the monochromatic beam. Positioning of the sample was done with two mutually perpendicular horizontal stages and one vertical stage. The horizontal stages were mounted on top of a vertical rotational stage aligned with the X-ray beam. The reproducibility of the translational stages and eccentricity of the rotational stage were less than $0.5\ \mu\text{m}$ and $1\ \mu\text{m}$, respectively. It should be noted that, in diamond anvil cell (DAC) experiments, strong reflections from diamonds can damage the detector during data collection. To block such reflections, we first

collected data at much reduced incident beam intensity, and then carefully placed lead pieces at all corresponding reflection locations on a Kapton foil just in front of the detector.

The sample was cut manually from a Si wafer (University Wafer¹⁸) parallel to (001) and had a thickness of $15 \pm 2\ \mu\text{m}$. The sample had a rectangular shape defined by cleavage planes parallel to [110] and size about $30 \times 60\ \mu\text{m}^2$. It was put into a DAC loaded with He as pressure medium, which provided essentially hydrostatic compression over the pressure range in this study. The data were collected using polar orientation of the DAC: both incident and diffracted beams passed through the diamonds.

Cell pressure was slowly increased using a gearbox and measured using an online ruby fluorescence system.¹⁹ As soon as the pressure reached 13.08 GPa, data collection using white beam started. In order to get spatially resolved structural information, a series of identical two dimensional (2D) grid scans was made as the pressure was increased up to 13.31 GPa. In each 2D grid scan, Laue diffraction images were collected at each step, with a step size of $5\ \mu\text{m}$ and an exposure time of 0.5 s. The 2D scan covers the whole sample area, providing spatially resolved crystallographic information as the Si sample underwent the phase transition. Collection of one 2D translational scan took 2.5 min and the total time of

data collection was 2 h and 7 min, resulting in a total of 23 2D Laue scans. After the data collection was finished, β -phase was visible in the Laue images and was later confirmed using the monochromatic beam.

Laue reflections from the sample have been indexed in two steps using software specifically developed for this purpose. At the first stage, orientation matrix of the sample was calculated previously using well known approach based on positions and indices of two monochromatic beam reflections collected before the 2D grid scans started.²⁰ Indices of these two reflections were available from their d -values. Range of possible indices of each observed Laue reflection from the sample was determined from the 2θ -angle of reflection, space group, and the X-ray energy range. Each possible combination of indices was used to predict a reflection position on the area detector. Those indices with the smallest deviation of the predicted position from the observed one were used for further analysis. At the second stage, all the observed Laue diffraction spots were finally indexed using the same approach but based on orientation matrix determined precisely from the known indices and positions of two strong Laue diffraction spots.²¹ Despite drop of photon flux at higher X-ray energies, multiple reflections having calculated energy values close to the highest limit of 70 keV were observed. The orientation matrices of different parts of the sample were determined this way during the phase transition to calculate angles between the crystal lattices using software routine developed for this purpose. The Fit2d peak search function was used to find the coordinates of reflections. In order to estimate the angular uncertainty of the orientation matrix and to recognize the presence of deviatoric strain during the phase transition, Laue diffraction data were collected on the starting material of the same Si wafer at ambient pressure. In total, six diffraction patterns containing 30–44 reflections have been recorded at different orientations, and the deviations between predicted and observed positions of diffraction spots were within a ~ 1 pixel limit which corresponds to an angular uncertainty of $\sim 0.02^\circ$. This provides an instrumental detection limit in measuring deviatoric strain of the sample under phase transition.

A typical Laue image is shown in Fig. 2(a). Areas on the images containing strong reflections from the diamonds were shaded by the lead pieces. Reflections from random crystalline particles present on the outer surfaces of the diamonds were masked and excluded from consideration. In order to extract spatially resolved structural information from a translational scan, regions around each Laue reflection were combined into a composite frame as a function of scan position using Fit2d in the same order as these images were collected. All these composite images have the same number of rows and columns with the same relative positions to the sample. Fig. 2(b) shows a typical composite image based on the reflection Si (391). These composite images carry detailed spatially resolved information on the morphology of the sample, lattice orientation, and strain fields and serve as the main source for characterizing microstructures of the sample. An optical image of the sample obtained immediately after the data collection was finished is shown in Fig. 2(c).

RESULTS AND DISCUSSION

Morphology of phases

The composite images allow real time observation of the morphology of both the parent and product phase areas. This approach can provide valuable information on the mechanisms of structural phase transitions and phase transformations. Its spatial resolution is limited by the beam size and step size of the translational scans. Improvement in the spatial resolution can be made using a more tightly focused beam and reduced step size, but this comes at the cost of increased time in scans and consequently reduced time resolution. In order to overcome this general challenge, it is useful to combine application of micrometer or submicrometer beam with a large beam. The former can be used to get high resolution morphology information over smaller areas, while the latter can be implemented to get such information over larger areas but with lower spatial resolution. Also for better time resolution, faster area detectors and translational stages should be considered. Spatial resolution of the considered experimental setup is limited by the beam size of $7\text{--}9\ \mu\text{m}^2$ while the translational stages allow submicrometer spatial resolution.

Different kinds of morphology information can be extracted from such composite images. For examples, crystallographic relations between parent and product phases can be determined.³ Idiomorphism of single-crystals with respect to polycrystalline phases may be recognized. When combined with the orientation matrix of a single-crystal, indices of its edges or faces may be found. Nucleation and growth type phase transitions may be distinguished from those close to martensitic. Intra crystalline phase transitions may be recognized. Correlation of product phase area shapes with the crystallographic directions of the parent crystal can be studied.

In the considered example of $\alpha \rightarrow \beta$ phase transition in Si, the studied area covered the whole sample. The first observed change of the sample, caused by the phase transition, was the splitting of reflections from the α phase and the appearance of strong diffuse reflections, typical of textured powders, from the β phase. Composite frames of all the observed reflections from the α -phase clearly indicate splitting of its original crystal to smaller crystals with slightly different orientations, while composite frames of the product phase reflections show that it was scattered and located in areas between those split parent crystals. Composite images of one of the reflections of the α -phase together with composite frames of the diffuse reflection of the β -phase from two consecutive translational scans just after the phase transition started are shown in Fig. 3. The morphology of the α - and β -phase areas is shown schematically in Fig. 4. Areas of β -phase were strongly elongated parallel to the $[\bar{1}10]$ direction of the parent Si crystal. At the same time, no elongation of the product phase areas in the perpendicular $[110]$ direction was observed, despite its equivalence to $[\bar{1}10]$. This indicates that nucleation and growth of the β -phase may have related with defects, possibly introduced during sample preparation.

Toward the end of the data collection, the sample consisted mainly of β -phase while the remaining α -phase

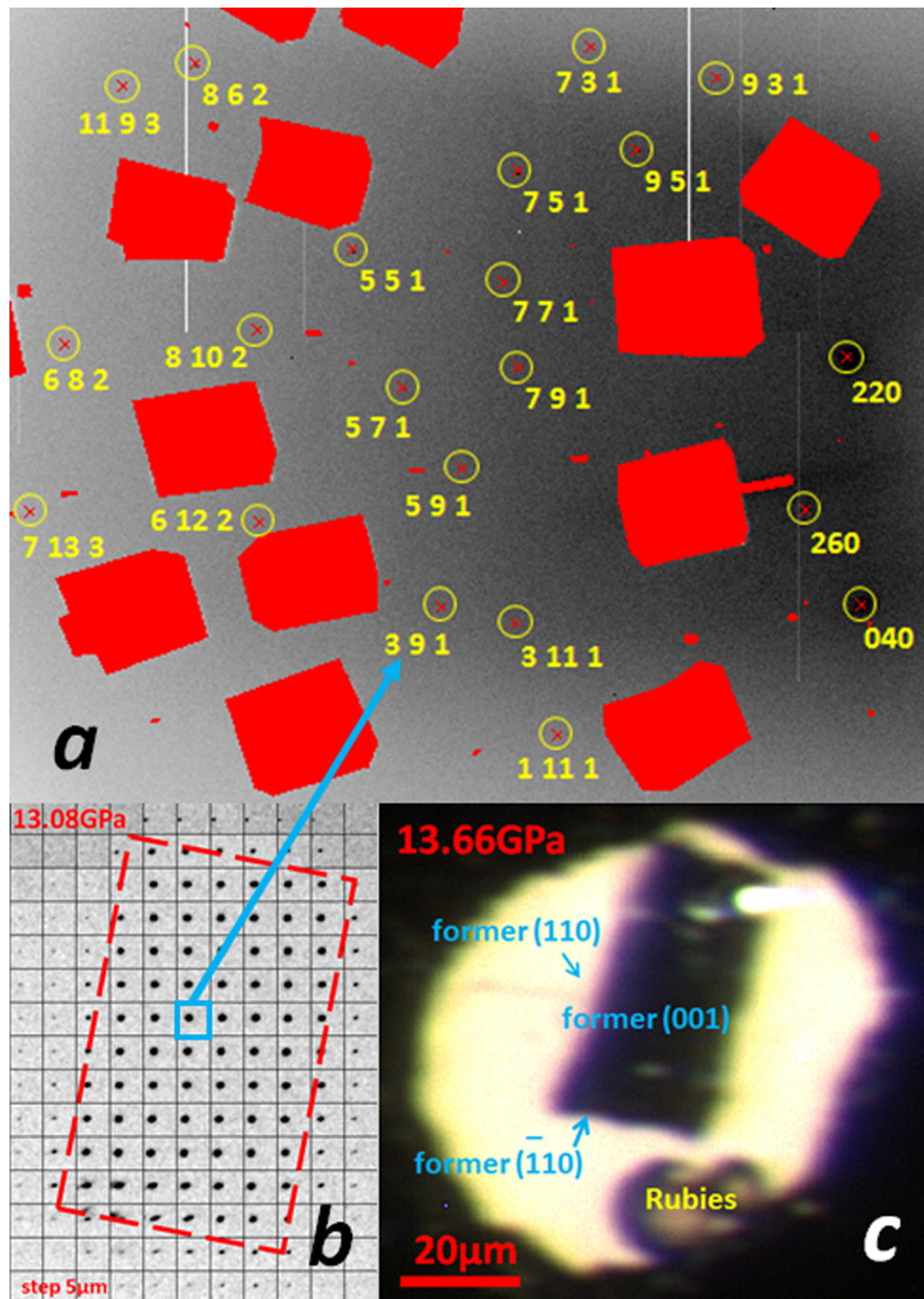


FIG. 2. (a) Typical diffraction pattern at a pressure just below the phase transition. Reflections from the α -phase single-crystal are denoted by red crosses and encircled. Indices correspond to the lowest observed orders of reflections. Areas which were masked are filled in red. These areas contained strong reflections from diamonds shaded by lead pieces and reflections produced by crystalline dust on the outer surfaces of diamonds. (b) Composite frame of Si (391) reflection from a translational scan collected at pressure right below the phase transition reproduces shape and orientation of the sample (outlined by red dotted line). (c) Optical image of the sample right after the data collection shows that the sample still keeps its original shape and orientation.

was still single-crystal with the same orientation as before starting data collection (Fig. 5). The residual α -phase area was strongly elongated in the original $[\bar{1}10]$ direction. The high pressure β -phase was further identified by the presence of its strong diffraction lines on X-ray images collected with the monochromatic beam. No attempts to index the diffuse white beam reflections from β -phase were successful due to two reasons. First of all, because these reflections were broad, uncertainty was introduced to their indices. Another reason was twinning of the high pressure phase indicated by

presence of crystallographic planes (211) and (220) parallel to each other (Fig. 5(c)). This made impossible to distinguish reflections from the same twin domain of β -phase.

A very incoherent interface between the α - and β -phases was observed: diffraction spots from the α -phase are sharp even as the phase transition nears completion, while reflections from the high pressure β -phase exhibit polycrystalline nature. This observation is in good agreement with the large volume collapse caused by the phase transition. An important advantage of this approach is that this contrast

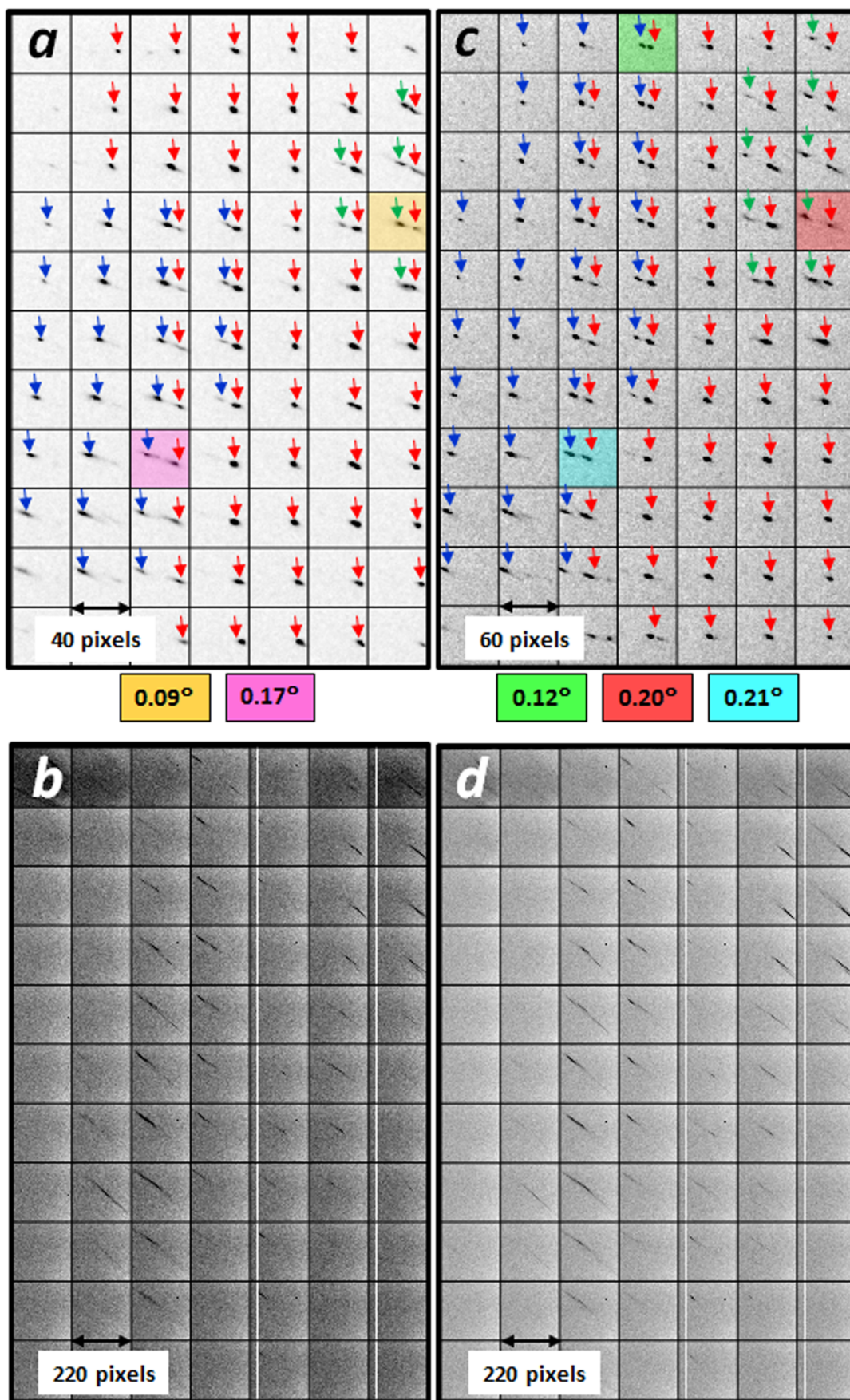


FIG. 3. (a) Composite frames of Si (862) reflection from the α -phase. (b) Polycrystalline reflection from the β -phase. Arrows denote reflections from crystal 1 (red), crystal 2 (blue), and crystal 3 (green) of α -phase. Angles between lattices of these crystals are shown in rectangles of the same colors as the corresponding parts of the composite images. Exactly the same composite frames from the next translational scan are shown in (c) (the same image as in (a)) and in (d) (the same image as in (b)).

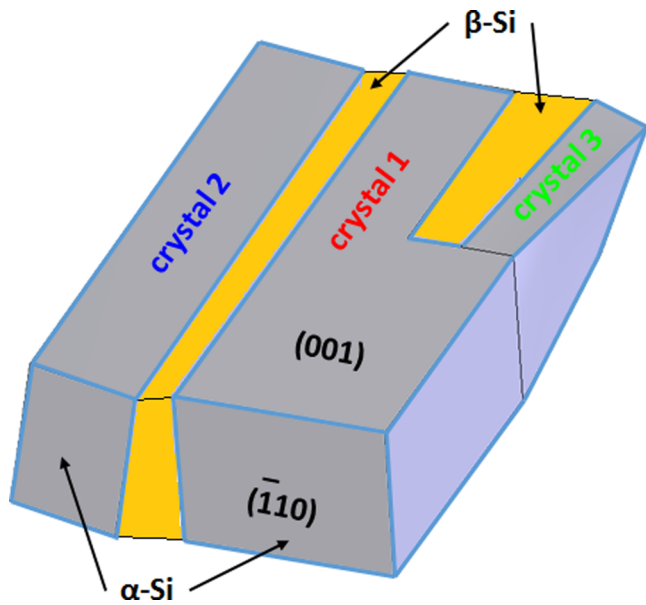


FIG. 4. Schematic of the appearance of the β -phase at the stage of the phase transition presented in Fig. 3. Crystal 1, crystal 2, and crystal 3 are the same as in Fig. 3 and denoted by the same colors. Crystals 2 and 3 are shown deformed assuming that they are twisted around their longest dimensions. Angles between the crystals are multiplied by a factor of 50.

can be clearly observed right at the interface between the α - and β -phases in a time-resolved manner. The current setup provides a time resolution of sub-second. Use of focused, monochromatic beam to probe the interface region would be problematic since there is a chance that the interface could change or move during the longer collection time required at each point on the sample. Monochromatic diffraction data may be collected at comparable speeds to the Laue method if the X-ray beam is large enough to cover the entire sample. However, this will wash out the spatial information and result in a poor signal to noise ratio for the diffraction from the interfacial area. The morphology of parent and product phase areas can be also studied *in situ* in real time with comparable spatial and temporal resolution by optical methods including Raman

spectroscopy.^{15,22–25} However, these methods cannot provide structural information directly because it can be obtained only based on known structure/optical property relations. These relationships are not readily obtained during phase transitions accompanied by a drastic change in the type of chemical bonding. Therefore, the developed Laue method provides unique spatially and temporally resolved information about the morphologies of various phases simultaneously with their structure data.

Relative orientation of single-crystals

Using the developed approach, orientations of single-crystals with respect to one another can be clearly determined in real time mode because multiple reflections from each of them can be recorded simultaneously in a short time interval. This can provide spatially and temporally resolved information on, for example, orientation relations between parent and product phases, deformation of single-crystals, and twinning or inter growth of crystals. The available level of angular precision of $\sim 0.02^\circ$ was enough to identify substantial variation of angles between the same crystals of α -phase over the sample which is an indication of deformation of these crystals as shown in Fig. 3. Angular uncertainty can be reduced by one order by doing a least square fitting of the orientation matrices against all the observed reflections. Precise measurement of angles between single-crystals requires recording of reflections corresponding to reciprocal vectors roughly perpendicular to the axis around which these crystals are tilted one from another. The Perkin-Elmer detector used in these measurements is of sufficient size to record several of such reflections for arbitrary orientations of the tilt axes.

An important characteristic of the interface between the phases is how quickly it is moving during the phase transition. The available spatial resolution did not allow measurement of the speed of the interface directly; however, its variation along the interface can be qualitatively estimated based on angular deviations between the crystals of α -phase. Without

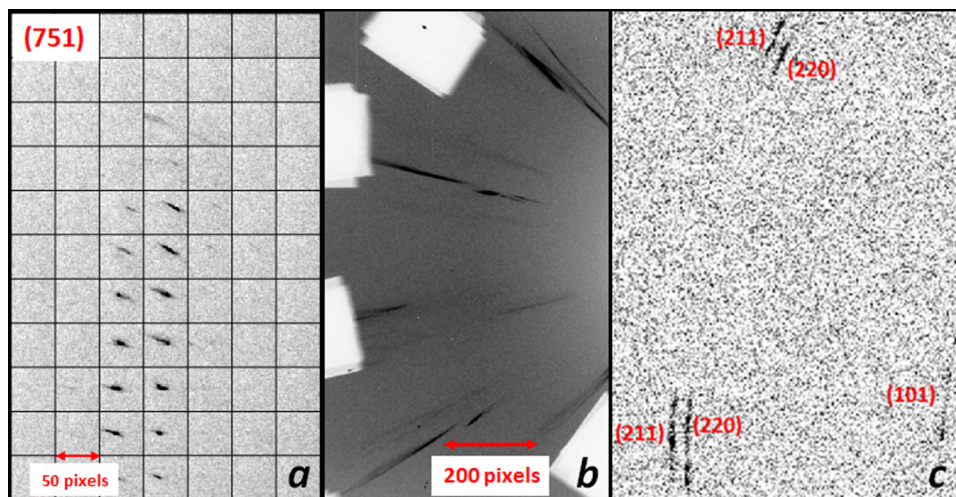


FIG. 5. Diffraction patterns at the end of data collection procedure. (a) Composite frame of Si (751) reflection from the rest of α -phase. (b) Typical Laue diffraction pattern from the β -phase. (c) Diffraction pattern from β -phase obtained using monochromatic beam. Indices of diffraction lines of β -phase are shown.

such variation, the crystals would stay parallel, but they would move towards each other with a speed defined by the linear contraction of $\sim 6\%$ accompanying the phase transition, provided the β -phase stays compact without cavities. If the rate of the phase transition changes along the interface, the high pressure phase areas are thicker when the speed is higher and the crystals of low pressure phase are moving faster towards to each other, defining their angular shift. The difference in contraction caused by the phase transition along the interface can be estimated based on average angles between the α -phase crystals and their sizes, but this would require precise knowledge of the orientations of the axes around which the crystals were tilted. As this information is not available, only a very rough estimate is possible yielding values in a range below 100 nm for crystals presented in Fig. 3(c) which in turn yield estimate of the differences of the β -phase areas thicknesses in a range below $1.7 \mu\text{m}$.

Deviatoric strain

The distortion of single-crystals caused by non-hydrostatic stress is characterized by the deviatoric strain tensor.²¹ It is detected by changes in the angles between reciprocal vectors with respect to an undistorted crystal. During pressure induced structural phase transitions or phase transformations, deviatoric strain can be present if there is a non-hydrostatic component of compression. It takes place at pressures higher than hydrostaticity limit of used pressure medium. Touching of the sample by both diamonds of a DAC during compression which is usually called “bridging” is another possible reason of deviatoric strain. If the sample consists of many grains, deviatoric strain can be caused by interaction of the grains with the diamonds and to each other. With the currently available ratio of pixel size over sample to detector distance, the precision of the deviatoric strain tensor components can be better than 3×10^{-4} which is comparable to other Laue diffraction dedicated facilities.²⁶ However, in order to approach this level of precision, one will need to do least squares fitting against at least 15–20 reflections. Even if this were to be done in the transmitted experimental geometry, only a limited number of reflections are available. The angles between their reciprocal vectors do not reflect precisely the deformation of the whole lattice which introduces additional uncertainty to the deviatoric strain. Calibration errors also contribute to the uncertainty. For the considered example of $\alpha \rightarrow \beta$ phase transition in Si, the deviation between the predicted and observed positions of reflections of ~ 1 pixel at pressures below the phase transition are indicative of deviatoric strain tensor components not higher than 5×10^{-3} and there is no indication of higher deviatoric strain of the α -phase during the phase transition. This showed that there was no “bridging” of the sample and that it was not squeezed by the gasket material and ruby balls during the phase transition.

Inhomogeneous strain in the α -phase parent crystals

An interesting result which may significantly improve the understanding of the mechanism defining the kinetics of the $\alpha \rightarrow \beta$ phase transition in Si was obtained by application of

the developed approach: lattice rotation of the α -phase single-crystals during the phase transition was observed. Reflections from the largest α -phase single crystal (crystal 1, denoted by red arrows in Fig. 3) stay at the same positions over a whole translational scan, while positions of reflections from crystal 2 (blue arrows in Fig. 3) and crystal 3 (green arrows in Fig. 3) exhibit continuous variation over a translational scan. This variation is reproducible over two consecutive translational scans presented in Fig. 3, which is an indication that this variation is caused by inhomogeneous strain in crystals 2 and 3 due to their lattice rotation and not by movements of these crystals with respect to crystal 1 during a translational scan.

The angles between the crystals shown in Fig. 3 together with dimensions of the sample provide some quantitative information about the lattice rotations of crystals 2 and 3. Proper analysis of this inhomogeneous strain would require determination of the orientations of the axes around which the crystals are tilted with respect to one another. Since the angles between the crystals were very small it would be challenging to calculate these directions precisely. Some qualitative estimates of these axes orientations are possible. All the observed reflections from crystals 2 and 3 exhibit deviations from the crystal 1 reflections in the radial direction, which is along the vector between the X-ray beam position on the detector plane and the reflection. This is an indication that the tilt axes are roughly perpendicular to the X-ray beam and parallel to the $[\bar{1}10]$ direction of the sample, which coincides with its longest dimension. In other words, crystals 2 and 3 appear to be “twisted” around their longest dimensions as is illustrated in Fig. 4.

One possible explanation of the inhomogeneous strain may be the interaction of crystals 2 and 3 with the β -phase areas located between them and crystal 1. It can be also related to the precursor phenomenon which was observed previously at lower pressures.¹¹ Clear explanation of the inhomogeneous strain requires further studies which can include theoretical modelling and diffraction measurements with micrometer or submicrometer beam in order to obtain information about precise orientation relations between the parent and product phases at their interfaces.

It is important to stress that recognition of inhomogeneous strain in α -phase single-crystals, and its quantification, would be much more challenging using monochromatic beam because collection of a sufficiently high number of reflections at each point in the sample would be much more time consuming due to the need for sample rotation. In particular, since the angles between these crystals were smaller than 0.21° , their measurement with monochromatic beam would require fine slicing. Substantial changes in this strain during the phase transition were observed over time intervals of a few minutes, while collection of one translational scan of the same resolution using monochromatic beam would take hours to days.

Future developments

One important future development of this technique will involve the use of micrometer or submicrometer X-ray beams to improve the spatial resolution. For the example of the $\alpha \rightarrow \beta$

phase transition in Si, this will allow measurement of spatially and temporally resolved structural information from the β -phase while similar data from the α -phase is still available. On the other hand, Laue measurements using larger beams, similar to what was used in this work, will be also needed in order to get information representative of the sample as a whole.

Although a 1- μm beam allows diffraction measurements on micrometer-sized crystalline grains, its application will face an obvious challenge due to the thickness of the sample, which will present multiple crystals grains along the beam direction, all of which will contribute to the diffraction images simultaneously. If the crystal grains under examinations have a size comparable to the X-ray beam, the number of crystals present in the beam will be on the order of tens which still will be acceptable for data analysis.²⁶ In the megabar pressure range, the thickness of the samples will be only a few micrometers, which will in fact simplify the data analysis.

Another important future development will be the implementation of 90° geometry using a panoramic DAC with a transparent gasket.⁴ Such an experimental setup will provide a much larger number of reflections which in turn will improve the precision of the deviatoric strain tensor and crystal orientation refinements.

In the considered case study, time resolution was mainly limited by the slow vertical translational stage; this will be easily improved in the future by using a faster elevation stage. After that, the resolution in time will be mainly constrained by the Perkin-Elmer area detector because it has readout time of 130 ms and because its sensitivity does not allow exposure times much shorter than 0.5 s. In 90° geometry, Pilatus 1M area detector having readout time of ~ 3 ms will be considered because it has much higher sensitivity in X-ray energy range below 25 keV applicable with such a setup.

High pressure high/low temperature studies using cryostats, resistive, or laser heating are also considered for future developments.

ACKNOWLEDGMENTS

The research was carried out at HPCAT, Carnegie Institution of Washington. High pressure Laue experiments were performed at the HPCAT beamline 16-BM-B, at the Advanced Photon Source (APS). HPCAT operations are

supported by DOE-NNSA under Award No. DE-NA0001974 and DOE-BES under Award No. DE-FG02-99ER45775, with partial instrumentation funding by NSF. Use of the gas loading system was supported by GeoSoilEnviroCARS and COMPRES, the Consortium for Materials Properties Research. The Advanced Photon Source is a U.S. Department of Energy (DOE) Office of Science User Facility operated for the DOE Office of Science by Argonne National Laboratory under Contract No. DE-AC02-06CH11357. We would like to acknowledge Dr. R. Barabash from Oak Ridge National Laboratory and Dr. J. Bernier from Lawrence Livermore National Laboratory for useful discussions.

- ¹G. E. Ice, J. W. L. Pang, R. I. Barabash, and Y. Puzyrev, *Scr. Mater.* **55**, 57 (2006).
- ²G. E. Ice and J. W. L. Pang, *Mater. Charact.* **60**, 1191 (2009).
- ³N. Li, Y. D. Wang, W. J. Liu, Z. N. An, J. P. Liu, R. Su, J. Li, and P. K. Liaw, *Acta Mater.* **64**, 12 (2014).
- ⁴G. E. Ice, P. Dera, W. Liu, and H. K. Mao, *J. Synchrotron Radiat.* **12**, 608 (2005).
- ⁵C. Nisr, G. Ribarik, T. Ungar, G. B. M. Vaughan, P. Cordier, and S. Merkel, *J. Geophys. Res.* **117**, 1, doi:10.1029/2011JB008401 (2012).
- ⁶S. Minomura and H. G. Drickamer, *J. Phys. Chem. Solids* **23**, 451 (1962).
- ⁷J. C. Jamieson, *Science* **139**, 762 (1963).
- ⁸J. Z. Hu, L. D. Merkle, C. S. Menoni, and I. L. Spain, *Phys. Rev. B* **34**(7), 4679 (1986).
- ⁹M. I. McMahon, R. J. Nelmes, N. G. Wright, and D. R. Allan, *Phys. Rev. B* **50**(2), 739 (1994).
- ¹⁰B. A. Weinstein and G. J. Piermarini, *Phys. Rev. B* **12**(4), 1172 (1975).
- ¹¹G. Shen, D. Ikuta, S. Sinogeikin, Q. Li, Y. Zhang, and C. Chen, *Phys. Rev. Lett.* **109**, 205503 (2012).
- ¹²H. Lorenz, B. Lorenz, and U. Kuhne, *J. Mater. Sci.* **23**, 3254 (1988).
- ¹³C. Dupas-Bruzek, T. G. Sharp, D. C. Rubie, and W. B. Durham, *Phys. Earth Planet. Inter.* **108**, 33 (1998).
- ¹⁴L. Kerschhofer, D. C. Rubie, T. G. Sharp, J. D. C. McConnell, and C. Dupas-Bruzek, *Phys. Earth Planet. Inter.* **121**, 59 (2000).
- ¹⁵N. V. C. Shekar and K. G. Rajan, *Bull. Mater. Sci.* **24**(1), 1 (2001).
- ¹⁶A. P. Hammersley, S. O. Svensson, M. Hanfland, A. N. Fitch, and D. Hausermann, *High Pressure Res.* **14**, 235 (1996).
- ¹⁷See <http://www.esrf.eu/computing/scientific/FIT2D/> for the software details.
- ¹⁸See <http://www.universitywafer.com/> for the vendor information.
- ¹⁹H. K. Mao, J. Xu, and P. M. Bell, *J. Geophys. Res.* **91**, 4673, doi:10.1029/JB091iB05p04673 (1986).
- ²⁰W. R. Busing and H. A. Levy, *Acta Crystallogr.* **22**, 457 (1967).
- ²¹J.-S. Chung and G. E. Ice, *J. Appl. Phys.* **86**(9), 5249 (1999).
- ²²Y. Okano and M. Nomura, *Jpn. J. Appl. Phys., Part 1* **28**(4), 696 (1989).
- ²³Z. A. Dreger and Y. M. Gupta, *J. Phys. Chem. B* **111**, 3893 (2007).
- ²⁴F. J. Lamelas, Z. A. Dreger, and Y. M. Gupta, *J. Phys. Chem. B* **109**, 8206 (2005).
- ²⁵G. J. Piermarini and S. Block, *Rev. Sci. Instrum.* **46**(8), 973 (1975).
- ²⁶N. Tamura, M. Kunz, K. Chen, R. S. Celestre, A. A. MacDowell, and T. Warwick, *Mater. Sci. Eng.: A* **524**, 28 (2009).